



## INTERESTING BEHAVIOR PATTERNS OF POROELASTIC BEAMS AND COLUMNS

G. CEDERBAUM,† K. SCHULGASSER and L. P. LI

Pearlstone Center for Aeronautical Engineering Studies, Department of Mechanical Engineering, Ben-Gurion University of the Negev, Beer Sheva 84105, Israel

(Received 21 April 1997; in revised form 20 January 1998)

**Abstract**—Unusual patterns in the time dependent behavior of the pore pressure in poroelastic solids (the Mandel–Cryer effect) were predicted and then observed over 25 years ago. Recently we formulated the problem of poroelastic beams dominated by axial diffusion, and results were found for several cases. It was observed that response peculiarities similar to those previously observed in massive structures are possible also for this case. We now show that not only are such unexpected results possible also for the deflection and slope, but that the time dependent patterns of all these variables may even be more complicated than in the case of the Mandel–Cryer effect. These interesting behavior patterns are qualitatively unobtainable with structures whose time dependent behavior results from modeling material behavior as viscoelastic. In this paper we present various behaviors of unusual nature exhibited by poroelastic beams and columns with axial diffusion.  
© 1998 Elsevier Science Ltd. All rights reserved.

### 1. INTRODUCTION

In a recent paper Abousleiman *et al.* (1996) re-examined the Mandel–Cryer (M–C) effect; they considered a generalized version of Mandel’s (1953) problem in which the material is transversely isotropic. Their complete solutions of stress, displacement and pore pressure established the M–C effect in this variation of the same basic problem, namely: a specimen, infinitely long in one direction and sandwiched between two rigid, frictionless plates, which is subjected to opposite and equal forces applied suddenly on the rigid plates; the lateral faces of the specimen are permeable to fluid. The M–C effect is the revelation of non-monotonic pore pressure response when a step loading is applied to a poroelastic body; after the initial pressure developed at the moment of application of the forces, the pressure at the center of the specimen continues to rise to a maximum before gradually decaying to zero. This is in contrast to the response which would be obtained within the traditional Terzaghi (1943) theory.

To the best of our knowledge, the M–C effect had not been observed in light poroelastic structures, such as beams, plates or shells. In a recently published paper by the present authors (Li *et al.*, 1995), behaviors similar to the M–C effect were discovered and discussed in the quasi-static response of beams in which fluid movement was possible in the axial direction only; the material of these beams was transversely-isotropic as we were motivated by consideration of plant stems and petioles. The results in that paper were obtained analytically by considering relatively “simple” cases of mechanical and diffusion boundary conditions. In order to investigate more general cases we developed a finite element code which enables us to perform analyses with vast combinations of the parameters involved, such as the variation of parameters along the beam axes, and having permeable or impermeable diffusion boundary conditions in any combination.

The first aim of this paper is finding behavior patterns of this kind (the M–C effect) in beams. The second aim is to display other kinds of interesting behavior patterns; these are mainly behaviors which differ qualitatively from the elastic and/or the viscoelastic counterparts. We limit ourselves, in this paper, to responses found for the quasi-static case of beams subjected to relatively simple loadings. Similar, or additional, unique behavior

† Author to whom correspondence should be addressed. Tel.: 00 972 7 6477075. Fax: 00 972 7 6472813.  
E-mail: gace@menix.bgu.ac.il

patterns are expected for plates (Li *et al.*, 1997a) and for vibration problems (Li *et al.*, 1996).

## 2. PROBLEM FORMULATION

Consider the beam shown in Fig. 1. Its moment of inertia with respect to the  $y$ -axis is  $I$ ; its cross-sectional area is  $A$  and is taken to be symmetric with respect to the  $z$  axis. The beam is subjected to a distributed normal load  $q_n(x, t)$  and a distributed axial load  $q_s(x, t)$ . The elastic porous matrix is saturated with a fluid, and the microstructure is such that the beam material is transversely isotropic and permits fluid movement only, or at least predominantly, in the axial direction; thus fluid velocities in the  $y$  and  $z$  directions are negligibly small compared to those in the  $x$  direction. We adopt the two assumptions which are the basis of classical beam theory for beams whose cross-sectional dimensions are small compared to length: (1) plane cross-sections of the beam remain plane after deformation, and (2) the only non-negligible normal stress is the  $x$  component of normal stress  $\tau_x$ , which is averaged over both solid and fluid phases. The constitutive law applicable to the transversely isotropic poroelastic beam under the assumption (2) is (see Li *et al.*, 1995)

$$\tau_x = E\varepsilon_x^s - \eta p_f, \quad \zeta = \eta\varepsilon_x^s + \beta p_f \quad (1a,b)$$

Here  $p_f$  is the fluid pore pressure,  $\zeta$  is the increment of fluid content in the pores, and  $\varepsilon_x^s$  is the axial normal strain in the solid skeleton. The physical meaning of the three constants in (1),  $E$ ,  $\eta$  and  $\beta$ , is as follows. If we take  $p_f = 0$  we are considering the drained material. Thus we immediately see that  $E$  is the axial Young's modulus of the solid skeleton (drained). Further we note that  $\eta$  is the constant by which  $\varepsilon_x^s$  must be multiplied in order to find the change in pore volume for the drained material stressed in the  $x$  direction. It is not at all clear that  $\eta$  must be positive, but it is to be expected that for practical materials  $\eta$  would indeed be positive. Finally  $\beta$  is the ratio of pore fluid increment to pore pressure when there is no axial strain. For later convenience, instead of using  $\beta$  a new parameter will be introduced as

$$\lambda = \frac{\eta}{E\beta} \quad (2)$$

This parameter can also be interpreted as follows. Consider a sample of the material for which the fluid is trapped, i.e. the material is "jacketed". Then  $\zeta = 0$  and we find from eqns (1) that

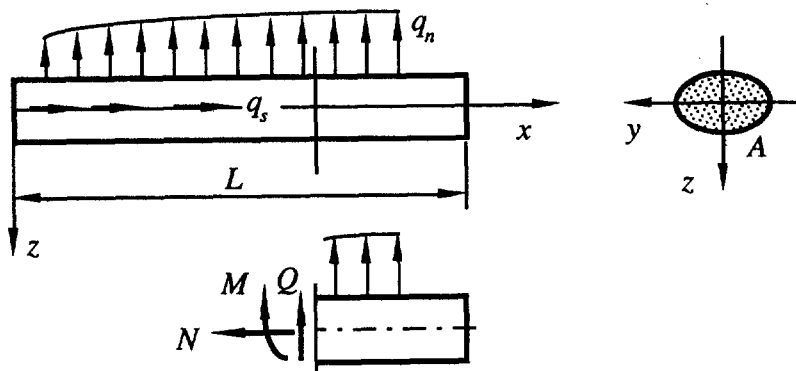


Fig. 1. Beam subjected to distributed normal and distributed axial loads, showing also the internal forces.

$$\tau_x = (1 + \lambda\eta)E\epsilon_x \quad (\zeta = 0) \tag{3}$$

In other words  $(1 + \lambda\eta)E$  is the Young's modulus of the bulk material when the fluid is trapped. This relationship is then applicable in relating stress to strain immediately after the application of suddenly applied loads. Clearly  $(1 + \lambda\eta)E > E$ , so we conclude that  $\lambda$  and  $\eta$  must have the same sign. We note that  $E$  and  $\eta$  are independent of the relevant mechanical property of the fluid, i.e. its compressibility.  $\lambda$  will depend both on the mechanical properties and microstructure of the skeleton, as well as on the fluid compressibility. Also when  $\zeta = 0$  we further record, for later use, another relationship,

$$p_f = -\frac{\lambda}{1 + \lambda\eta}\tau_x \quad (\zeta = 0) \tag{4}$$

Using the first of the above assumptions of beam theory it can be shown that when a beam element experiences an axial force  $N$  and/or a bending moment  $M$

$$N = EAu_{,x} + \eta N_p, \quad M = -EIw_{,xx} + \eta M_p \tag{5a,b}$$

where  $u$  and  $w$  are the axial and transverse displacements on the beam axis, the comma denotes  $x$ -direction derivatives, and

$$N_p = -\int_A p_f dA, \quad M_p = -\int_A p_f z dA \tag{6a,b}$$

are the pore pressure resultant and moment resultant over the cross-section. The equilibrium equations for the quasi-static case are then found to be

$$EA\frac{\partial^2 u}{\partial x^2} + \eta\frac{\partial N_p}{\partial x} + q_s = 0, \quad EI\frac{\partial^4 w}{\partial x^4} - \eta\frac{\partial^2 M_p}{\partial x^2} + q_n = 0 \tag{7a,b}$$

We now add relations involving fluid flow. Using Darcy's law with fluid motion only in the axial direction we have

$$\dot{\zeta} = \frac{k_{11}}{\mu_f}\frac{\partial^2 p_f}{\partial x^2} \tag{8}$$

where  $k_{11}$  is the axial permeability and  $\mu_f$  is the fluid viscosity. This enables us to express the fluid flow in terms of the global quantities  $N_p$  and  $M_p$  as follows

$$K\frac{\partial^2 N_p}{\partial x^2} - \dot{N}_p + \lambda EA\frac{\partial \dot{u}}{\partial x} = 0, \quad K\frac{\partial^2 M_p}{\partial x^2} - \dot{M}_p - \lambda EI\frac{\partial^2 \dot{w}}{\partial x^2} = 0 \tag{9}$$

where

$$K = \frac{k_{11}}{\mu_f\beta} \left( = \frac{k_{11}\lambda E}{\mu_f\eta} \right) \tag{10}$$

Boundary conditions on displacement for the axial problem are that  $u$  is given at certain points on the beam, possibly as a function of time; for the bending problem the displacement  $w$  and/or the angle  $\theta$  may be specified. Mechanical boundary conditions for the axial problem are that  $N$  is given at certain points, and for the bending problem  $M$  and/or  $Q$  are specified. For a permeable end surface the boundary condition is that  $p_f$  is given; in terms of pore pressure resultants this means that  $N_p$  and  $M_p$  are given. For an

impermeable end surface the derivative of  $p_f$  with respect to  $x$  is zero, hence the  $x$  derivatives of  $N_p$  and  $M_p$  are zero.

In order to determine the initial conditions, we must consider the situation when the load is suddenly applied, i.e. a jump at  $t = 0^-$ . Then at  $t = 0$ , we have  $\zeta = 0$  and the relationships (3) and (4) apply. From (3) we immediately see that the instantaneous response of the beam is that for an elastic beam of Young's modulus  $(1 + \lambda\eta)E$ . Then  $u(x, 0)$  and  $w(x, 0)$  are easily calculated and we can find  $N(x, 0)$  and  $M(x, 0)$ . (If the problem is statically determinate these would be known *a priori*.) Then integrating (4) over the area, and also after first multiplying by  $z$ , we have

$$N_p = \frac{\lambda}{1 + \lambda\eta} N, \quad M_p = \frac{\lambda}{1 + \lambda\eta} M \quad (t = 0) \quad (11a,b)$$

These can be given in terms of the displacements

$$N_p = \lambda EA \frac{\partial u}{\partial x}, \quad M_p = -\lambda EI \frac{\partial^2 w}{\partial x^2} \quad (t = 0) \quad (12a,b)$$

determining the pore pressure resultant and moment resultant at  $t = 0$ .

We point out that if  $\lambda$  and  $\eta$  are zero (if  $\lambda = 0$  then  $\eta = 0$ , and vice versa), the corresponding equations will degenerate to those for an elastic beam.

Finally we note that for a beam of length  $L$  sealed at both ends, i.e. no fluid can be lost, one can show that for all times

$$\int_L \frac{\eta}{E} \left( \frac{1 + \lambda\eta}{\lambda} N_p - N \right) dx = 0, \quad \int_L \frac{\eta}{E} \left( \frac{1 + \lambda\eta}{\lambda} M_p - M \right) dx = 0 \quad (13a,b)$$

At long times the pore pressure resultant and moment resultant reach constant values; then if  $\lambda$ ,  $\eta$  and  $E$  are constant along the beam these long time values are given by

$$N_p^\infty = \frac{\lambda}{1 + \lambda\eta} \frac{1}{L} \int_L N dx, \quad M_p^\infty = \frac{\lambda}{1 + \lambda\eta} \frac{1}{L} \int_L M dx \quad (14a,b)$$

### 3. RESULTS AND DISCUSSION

Analytical solutions for this problem were established in Li *et al.* (1995) for relatively simple cases such as simple-supported or cantilever beams. However, it is not possible to solve all cases analytically due to the complexity of the partial differential equations and the relevant boundary conditions governing the problem; a numerical scheme is required. A finite element formulation for the problem under consideration was developed in Li *et al.* (1997b). The high accuracy of the numerical scheme was demonstrated by comparison with the previously found analytical solutions, and the influence of grid size on the rapidity of convergence to the correct solutions was examined. These solution procedures will not be presented herein, but we emphasize that their accuracy has been clearly shown in the above referenced works.

The cases we wish to show can be divided into two groups: (1) those associated somehow with the Mandel–Cryer effect, and (2) those associated with structural behaviors which differ qualitatively from the elastic and/or viscoelastic counterparts. In all cases the loads are considered to be applied suddenly and remain constant thereafter.

The relevant quantities will be displayed in nondimensional form, as follows

$$\begin{aligned}
 x^* &= \frac{x}{L}, & t^* &= \frac{Kt}{L^2}, & q_s^* &= \frac{q_s L}{EA}, & q_n^* &= \frac{q_n L^3}{EI}, & u^* &= \frac{u}{L}, \\
 w^* &= \frac{w}{L}, & N_p^* &= \frac{N_p}{EA}, & N^* &= \frac{N}{EA}, & M_p^* &= \frac{M_p L}{EI}, & M^* &= \frac{ML}{EI}
 \end{aligned}
 \tag{15}$$

For the sake of simplicity, when presenting results, the superscript \* will be omitted. And further, “pore pressure” will be used to refer to  $M_p$  since this variable has the same distribution as for pore pressure in terms of  $x$ . Note that after the normalization only two material parameters,  $\lambda$  and  $\eta$ , will appear in the computations. When  $\lambda = \eta = 0$  we return to the elastic case; the more  $\lambda$  and  $\eta$  deviate from 0 (especially their product) the greater is the poroelastic effect. The qualitative features of the behavior patterns to be presented below are not dependent on the magnitudes of  $\lambda$  and  $\eta$ . However, for the sake of the visual display in the graphical representation of the behavior patterns we will choose relatively large values of  $\lambda$  and  $\eta$ . We do not enter into the question of what values of these parameters might be appropriate for such materials which can be readily fabricated. But we emphasize that the values to be chosen are all theoretically realizable. We have chosen throughout  $\eta = 1$ ; it is easy to postulate micro-structures for which this value is attainable when the transverse stiffness of the drained material is very high compared to the axial stiffness. Large values of  $\lambda$  then simply imply high bulk modulus of the pore fluid compared to the axial elastic stiffness of the skeletal material.  $\lambda$  has been chosen in the various examples as either one or six. Again we emphasize that the behavior patterns to be displayed are not qualitatively dependent on the magnitudes chosen for  $\lambda$  and  $\eta$ .

We first consider the case of a cantilever beam subjected to a uniformly distributed load. (See the Appendix for details of this and all other cases of loading to be considered; the values of  $\lambda$  and  $\eta$  used are also shown.) Figure 2 shows the variation of pore pressure with time at the quarter, half, and three-quarter points along the beam; all possible combinations of diffusion boundary conditions are considered, i.e. permeable both at the wall and at the free end (P-P), permeable at the wall and impermeable at the free end (P-I), impermeable at the wall and permeable at the free end (I-P), and both ends impermeable (I-I). We see that for most positions and diffusion boundary conditions the pore pressure, after taking on its initial value immediately after application of the load (eqn (11b)), rises to some maximum value before decaying to zero. This is the pattern of pore pressure response at the center of the specimen in Mandel’s problem. For the I-I case the effect is discernible, but only barely so, for the quarter position. Of course, in this case the long time pore pressure is not zero; it approaches the value obtained from eqn (14b). Here we note that the pore pressure approaches its final value from above or from below depending on the position on the beam being examined. A physical explanation for a Mandel-Cryer type pore pressure pattern in the present problem is as follows. Consider the mid-point curves in Fig. 2a. At  $t = 0$  pore pressure is higher to the left of the mid-point than to the right of it. Thus the pressure differential is forcing fluid toward the right, and the immediate response is a rise in pore pressure at the mid-point. This is seen in all four cases of diffusion boundary conditions; the initial rates of pore pressure rise are identical. However, in cases (a) and (b) for which the left end (higher initial pore pressure) is permeable, the high pressure is quickly dissipated and the rise is quickly halted. In case (c), on the other hand, where the left end is impermeable, no loss of fluid on the left is possible and the pressure differential continues driving the process for a longer time, until finally fluid loss on the right end dominates the process, and the pressure decays toward zero. In case (d), where both ends are impermeable, no fluid loss on the right is possible and an asymptote is quickly reached.

The level of complexity which the pore pressure-time behavior can reach is shown in the next example. Figure 3 presents such behavior for a beam fixed at both ends; again the loading is uniform, and we again consider all possible combinations of diffusion boundary conditions. We examine the behavior at the three-quarter point. Because of the early time complexity we also give on the right an expanded version for the shorter times. In all cases

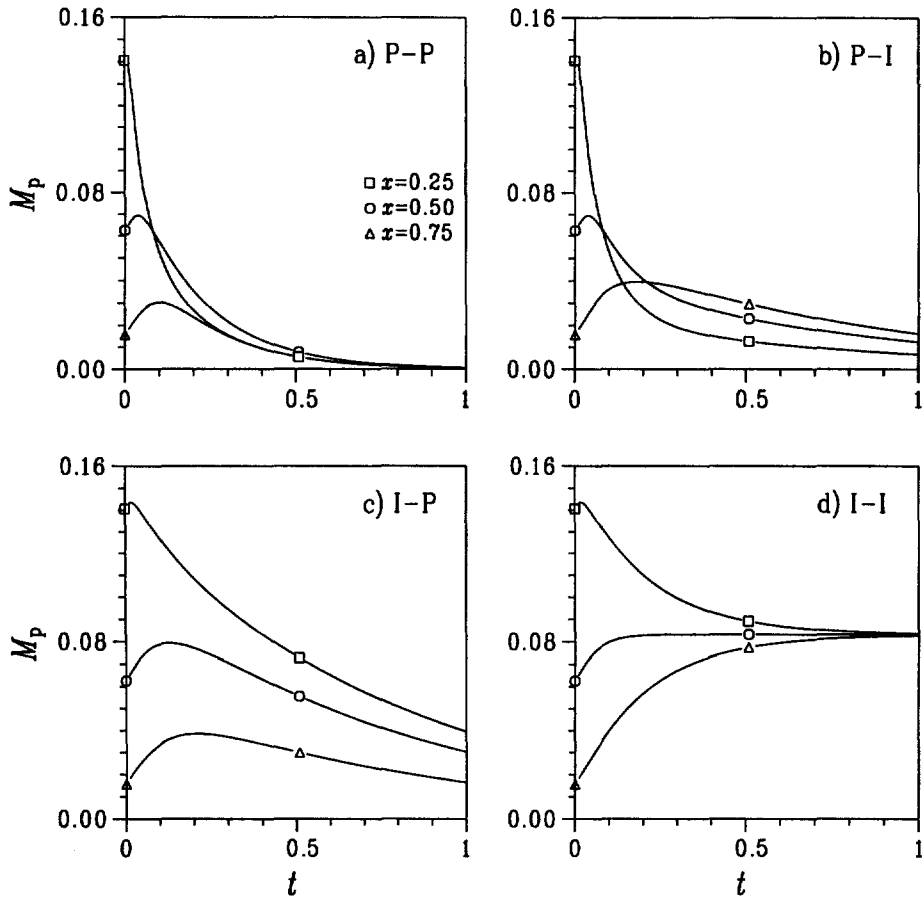


Fig. 2. Variation of pore pressure with time at the quarter, half, and three-quarter points along a cantilever beam subjected to a uniformly distributed load, for the various diffusion boundary conditions.

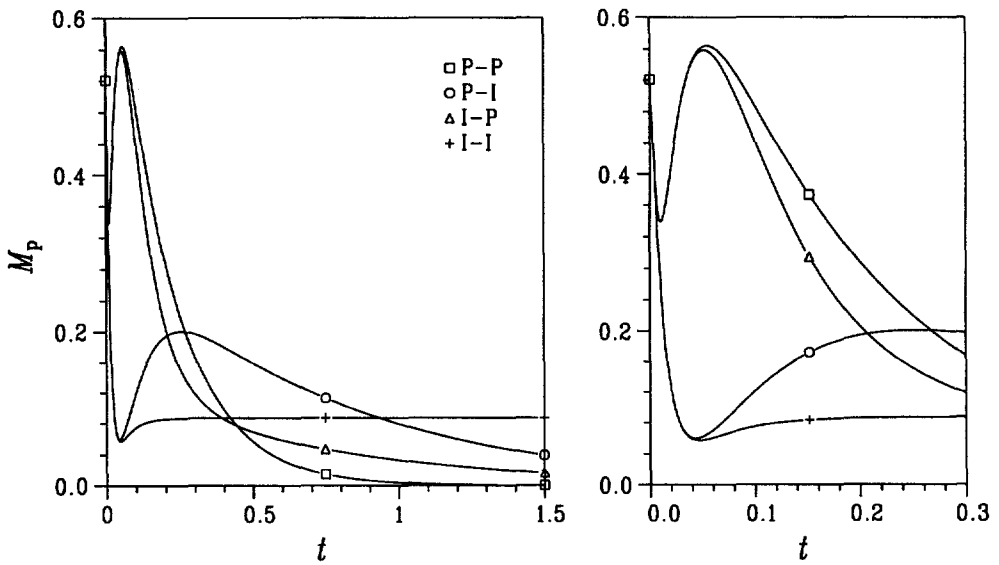


Fig. 3. Variation of pore pressure with time at the three-quarter point of a beam fixed at both ends for all possible combinations of diffusion boundary conditions; the loading is uniform. The short time portion is also shown expanded.

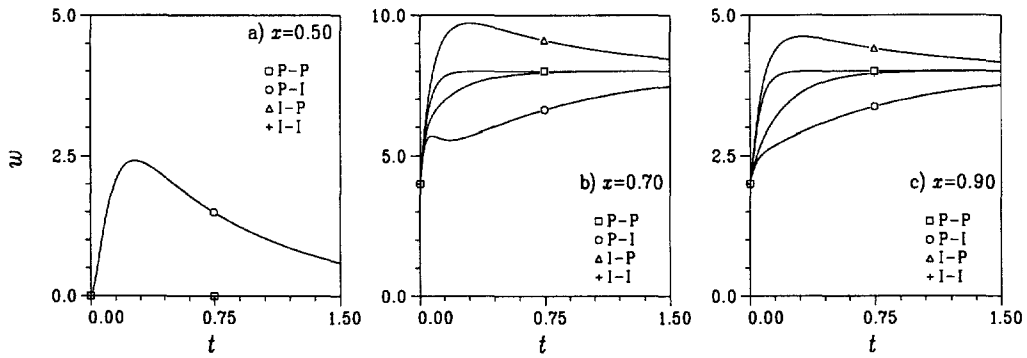


Fig. 4. Variation of deflection with time for a simply supported beam to which is suddenly applied a concentrated moment at the mid-point (a) At the mid-point,  $x = 0.5$ , (b) at  $x = 0.70$ , (c) at  $x = 0.90$ ; all four diffusion boundary conditions are shown.

the pore pressure initially falls from its value at  $t = 0$ —but then in each case the trend reverses and there is a subsequent pressure rise! And then for all cases when at least one end is permeable, the pressure again falls until it is completely dissipated.

That the anomalous behavior observed above (non-monotonic) can extend also to the deflection of the beam is shown in our next example. We consider a simple supported beam with a suddenly applied concentrated moment at the mid-point. All four diffusion boundary conditions are considered. Figure 4a shows mid-point deflection. When the diffusion boundary conditions are symmetric (P-P or I-I) and the loading is antisymmetric, the mid-point remains stationary. But when they differ (I-P or P-I) we observe anomalous behavior. Clearly at  $t = 0$  and at  $t = \infty$  the deflection must be zero; but at intermediate times we have a relatively quick rise to a maximum and then a decay to zero. Away from the mid-point even stranger behavior is observed. At  $x = 0.7$  with the P-I diffusion condition the deflection reaches a maximum, then drops, and then rises again to its asymptotic value. For the other asymmetric diffusion condition, I-P, the deflection behavior is always non-monotonic, but with only a single extremum. With symmetric diffusion boundary conditions the deflection is always monotonic, approaching its asymptotic value from below. At  $x = 0.9$  the phenomenon of two local extrema does not exist, but otherwise the behavior is similar to that at  $x = 0.7$ .

We now illustrate a completely different type of irregularity, which is outside of the scope of phenomena observed for the elastic or viscoelastic counterpart. Consider a cantilever as in Fig. 2, except that now only the left half of the beam (nearer the wall) is loaded. For the elastic or viscoelastic case it is obvious that the unloaded portion of the beam remains straight (no curvature). This is not the case in the present instance. After the initial response, for which the unloaded portion indeed remains straight, curvature begins to appear in this portion due to the existence of pore pressure throughout the entire length of the beam; see Fig. 5. If at least one of the beam ends is permeable, then the unloaded portion will finally be straight again since the pore pressure ultimately vanishes. In case (d), where both ends are sealed and the final value of the pore pressure is non-zero (eqn (14b)), some curvature remains for all times in the unloaded portion and its sign is opposite in sense to that in most of the loaded portion. Thus the beam tip deflection is for all times less in this case (I-I) than for the instances when at least one end is permeable. Note also that cases (a) and (b), for which the clamped end is permeable, behave quite differently from case (c) for which the clamped end is impermeable; after the initial response the deflection quickly approaches very nearly to its final value, while in (c) the change is more equally distributed in time.

The above loadings might be considered analogous to examining the creep behavior of a viscoelastic structure. Suppose we now examine the analogy of the relaxation behavior; i.e. we ask what will happen if we suddenly impose a deflection at some point, which is then held constant. We consider an unloaded cantilever beam at the free end of which a unit

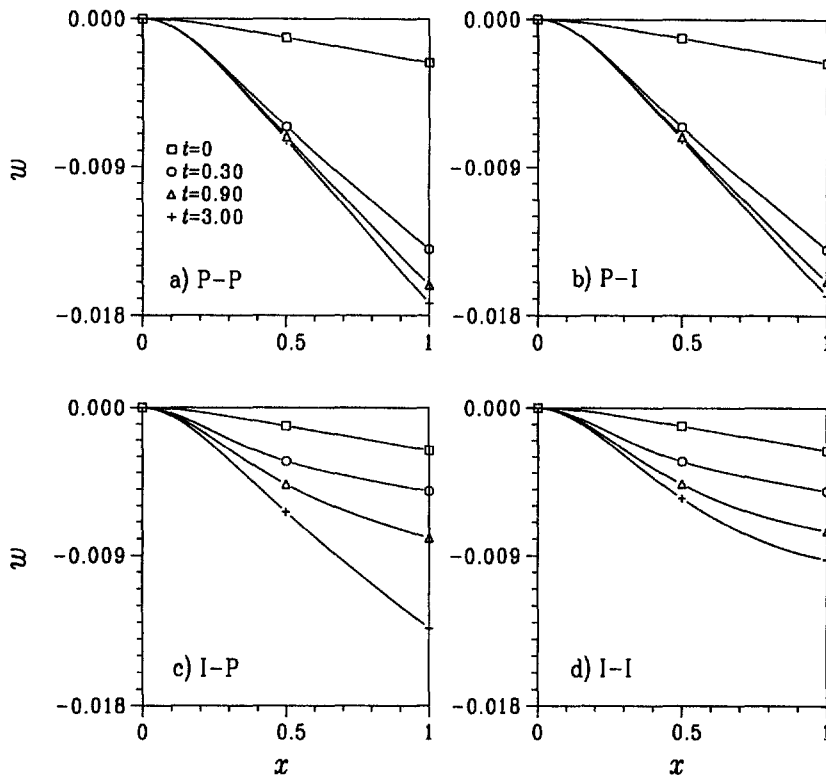


Fig. 5. Deflection vs position for various times for a cantilever beam loaded by a uniformly distributed load on its left half (closer to fixed end); all four diffusion boundary conditions are shown.

deflection is suddenly applied. The subsequent deflections along the beam for all diffusion boundary conditions are shown in Fig. 6. We see that the gross shape of the beam itself varies with time. This is qualitatively different from the behavior in the viscoelastic case; in that case the shape remains unchanged and only the internal stress is time dependent. The initial ( $t = 0$ ) shapes for all cases are the same and are identical to the shape for the elastic and viscoelastic cases, and these are in turn identical to the long time ( $t = \infty$ ) shape for all cases for which at least one end is permeable. But the long time behavior for the I-I case is again deviant. Here at all points along the beam the deflection increases monotonically with time. In fact for  $x > 0.85$  the final deflection is even greater than unity, resulting in a truly surprising shape. Now, in Fig. 7a we plot the deflection angle (slope),  $\theta$ , vs time at  $x = 0.5$  (and a magnified version for the shorter times,  $0 \leq t \leq 1.5$ ) for the same loading case. Here again, non-monotonic curves are obtained, and this in the complicated form of a double variation. When the clamped end is permeable there is a reduction in the angle at short times, then an increase, followed by a slow reduction towards the initial value obtained at  $t = 0$ . The I-P case has the same tendency, but the angle change is more moderate. Thus we note Mandel-like behavior with respect to another (third) variable. The I-I case seems to show the simplest behavior here, monotonic. But if we consider the point  $x = 0.95$ , i.e. very close to the displaced end, then we again see a manifestation of the truly unusual behavior in this case (Fig. 7b). The angle actually changes sign before finally reaching its asymptotic value. For points even closer to the displaced end the long time slope would be even more negative.

Finally, we consider the axial deflection of a column subjected to a uniformly distributed vertical load suddenly applied. In Fig. 8 the vertical deflection,  $u$ , vs the vertical location,  $x$ , is shown for all diffusion boundary conditions, at several times. When the top is permeable [cases (a) and (c)] the axial deflection is monotonic both with respect to location and with respect to time; this is as expected. When both ends are permeable the



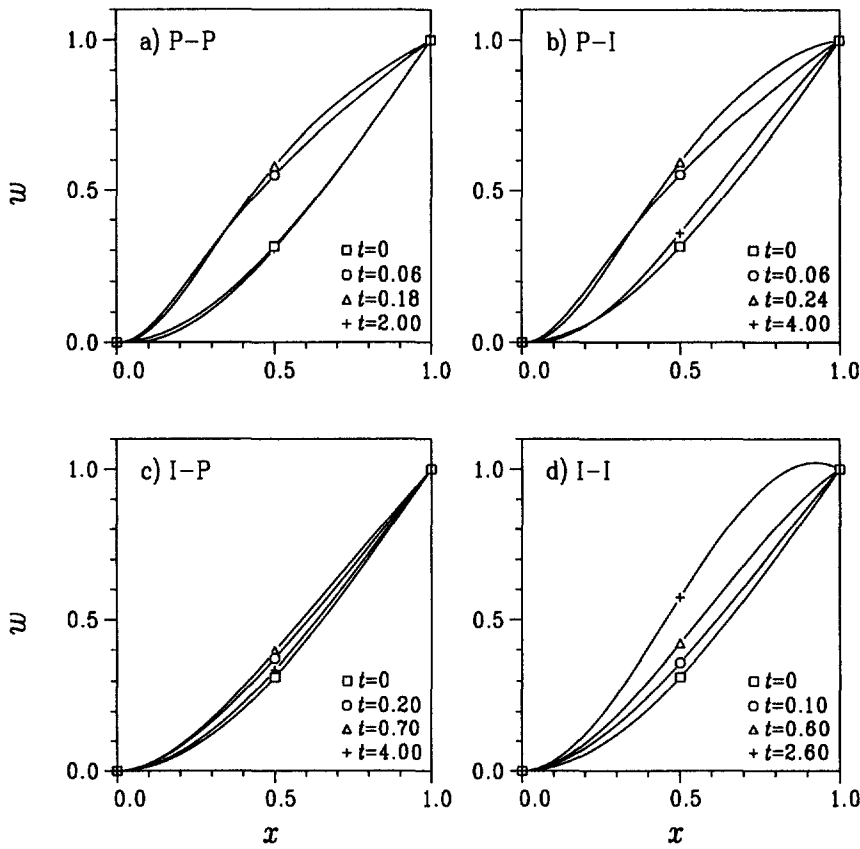


Fig. 6. Deflection vs position for various times for an unloaded cantilever beam to whose free end a sudden unit deflection is applied and then held constant; all four diffusion boundary conditions are shown.

long time downward deflection of 0.5 at the top is very nearly achieved at  $t = 1$ , while when the column base is impermeable, case (c), the final deflection [essentially that shown for  $t = 1$  in case (a)] is not achieved until much longer times. Now when the top end is impermeable [cases (b) and (d)], then while  $u$  is monotonic with respect to time it is not monotonic with respect to position. We see that in the upper portion of the column  $\partial u/\partial x$  may be positive; higher material points in the column deflect less than lower material points. Thus the skeletal material of the column is under tension in some regions. Moreover, when both ends are sealed, case (d), the immediate (at  $t = 0$ ) axial deflection at the top of the column does not change at all with time. That this must be so is shown as follows. Eliminating  $N_p$  from eqn (13a) using (5a) we have for all time

$$\int_L \frac{1}{\lambda E} [N - (1 + \lambda\eta)EAu_{,x}] dx = 0 \tag{16}$$

Now if the material parameters  $\lambda$ ,  $\eta$  and  $E$  are constant along the length of the column

$$u(L, t) = u(0, t) + \frac{1}{EA(1 + \lambda\eta)} \int_0^L N dx \tag{17}$$

But  $u(0, t)$ , the deflection at the base, is zero, and clearly the integral on the right is a constant in time; so  $u(L, t) = \text{constant}$ . In fact, since for any load distribution the integral on the right is independent of time, we can conclude that for any such loading the top of the column remains motionless.

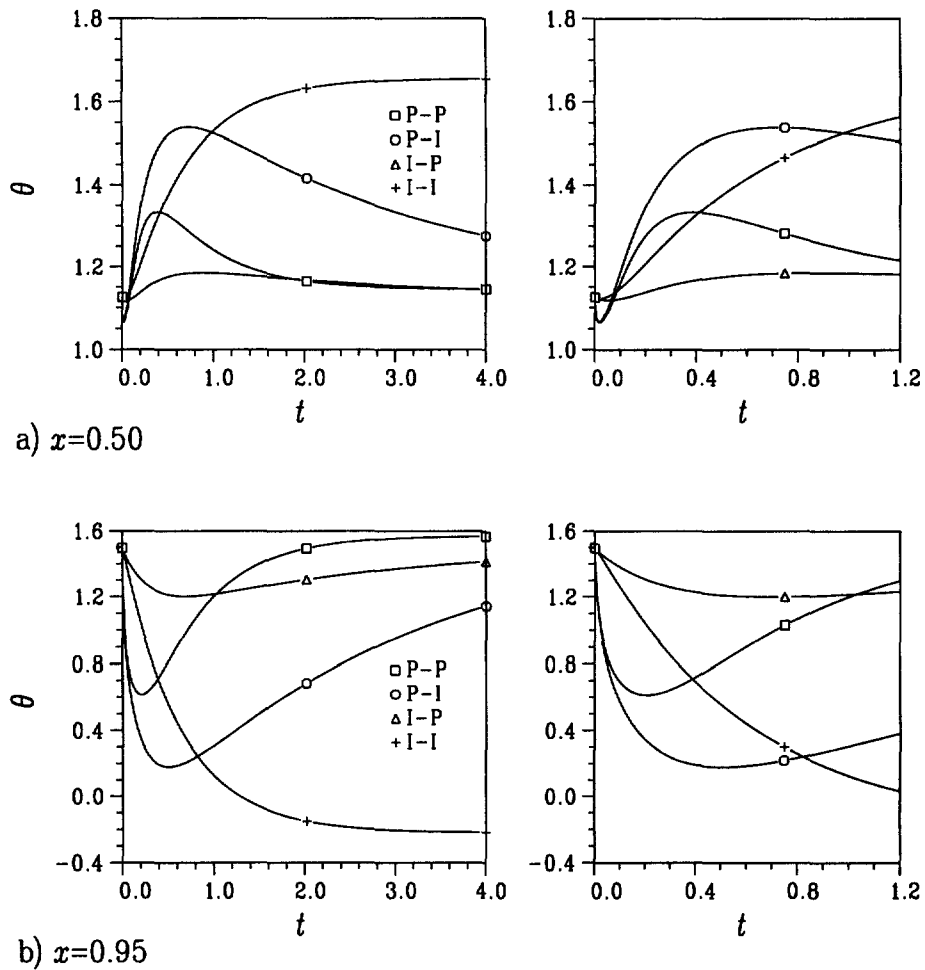


Fig. 7. Deflection angle vs time for the conditions of Figure 6; (a) at  $x = 0.5$ , (b) at  $x = 0.95$ . All four diffusion boundary conditions are shown. The short time portions are also shown expanded.

The situation we just considered is when  $\lambda$  and  $\eta$  are uniform along the length of the column (both equal 1). These are the physical parameters which were not taken out of the computation when normalizing. If these parameters vary then we cannot deduce (17) from (16), and there is no reason to expect that the top of the column will remain stationary. As an example, suppose  $\lambda$  is different (but constant) in the upper half of the column from in the lower half, while  $\eta$  (and  $E$  and  $K$  which were included in the normalization) remains constant along the entire column. It is possible to accomplish this by changing only the microgeometry and elastic properties of the solid skeleton, while the pore fluid is maintained uniform throughout. We examine how this influences the column's response for the I-I case. Take  $\eta = 1$  (as previously) throughout the column. Three cases will be considered: (a)  $\lambda = 6$  throughout; (b)  $\lambda = 1$  in the upper half while  $\lambda = 6$  in the lower half; and (c)  $\lambda = 6$  in the upper half while  $\lambda = 1$  in the lower half. The vertical deflections,  $u$ , vs the vertical location,  $x$ , are shown in Fig. 9 for all three cases, at several times. The results are surprising. In case (a) where  $\lambda$  is uniform there is no qualitative difference from the previous example; again we note that the immediate axial deflection at the top of the column does not change at all with time. However, the relative portion of the column where the skeleton is in tension is greatly increased. That this should be so is shown as follows.  $u$  reaches its maximum value when  $u_x = 0$ . From (5a) we see that this requires

$$N = \eta N_p \quad (18)$$

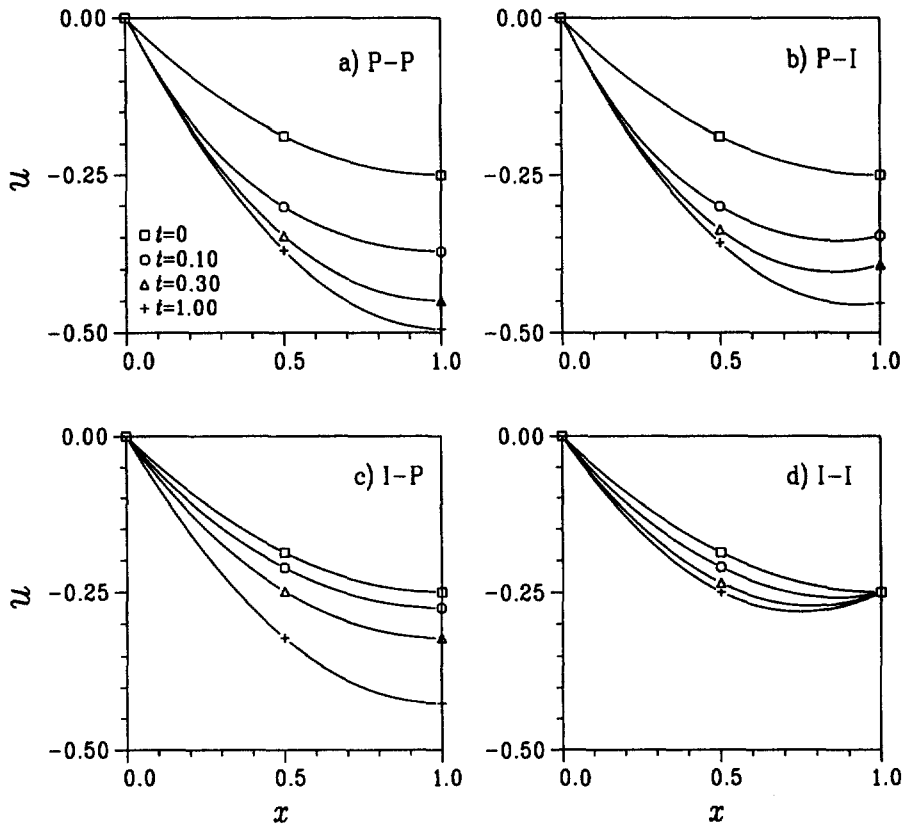


Fig. 8. Axial deflection vs position at various times, for a column subjected to a uniformly distributed load, all four diffusion boundary conditions are shown.

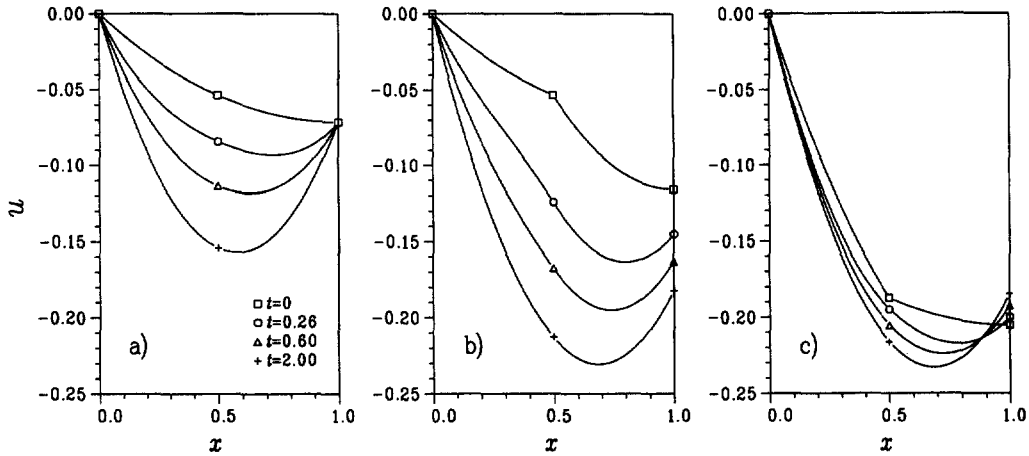


Fig. 9. Axial deflection vs position, at various times, for a column subjected to a uniformly distributed load, for I-I diffusion boundary conditions: (a)  $\lambda = 6$  throughout; (b)  $\lambda = 1$  in the upper half and  $\lambda = 6$  in the lower half; (c)  $\lambda = 6$  in the upper half and  $\lambda = 1$  in the lower half.

Now  $N$  is simply

$$N = -q(L-x) \tag{19}$$

while at  $t = \infty$  we calculate from (14a)

$$N_p = -\frac{\lambda}{1+\lambda\eta}q\frac{L}{2} \quad (20)$$

Inserting (19) and (20) into (18) we find that the position at which  $u$  is maximum is given by

$$\hat{x} = \frac{1 + \frac{1}{2}\lambda\eta}{1 + \lambda\eta}L \quad (21)$$

So any increase in the product  $\lambda\eta$  lowers the position on the column at which the maximum deflection is found; in our case this position has been lowered from  $\frac{3}{4}L$  to  $\frac{4}{7}L$ . Now in case (b) where  $\lambda$  in the upper part has the smaller value, we note that the initial deflection at the top of the column continues to grow in time to its final value. But in case (c) where the upper  $\lambda$  is the greater one, a very peculiar behavior is observed. After the initial (at  $t = 0$ ) downward deflection of the top of the column, this region of the column reverses its direction and moves upward until reaching its final position!

#### 4. CLOSURE

It has been shown in this paper that very unusual behaviors are possible in beams and columns made of poroelastic material which allows only axial diffusion. Bending of poroelastic beams has been considered in the past (e.g. Nowinski and Davis, 1972; Zhang and Cowin, 1994). But previous work considered materials for which fluid movement was possible in all directions. Stress gradients are generally overwhelmingly greater in the direction perpendicular to the beam axis than in the axial direction; therefore the axial fluid movement was considered negligible *vis à vis* the perpendicular movement. Thus fluid movement at a station along the beam is determined only by the bending moment in the beam at that station. Hence, in a statically determinate beam the fluid movement at any particular station is unaffected by the fluid movement at other points along the beam. For statically indeterminate beams the fluid movement at a particular station is affected only through the influence on the local bending moment at that station. In the present situation, i.e. beams made of material for which fluid motion perpendicular to the axis is suppressed, the diffusion behavior at any point on the beam is directly influenced by the situation along the entire beam, and thus also by the diffusion conditions at the beam ends. This is the basis for the unusual behavior patterns discovered.

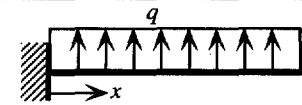
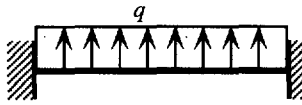
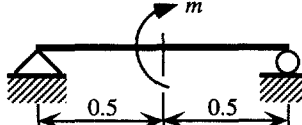
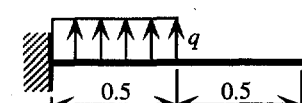

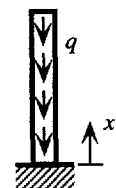
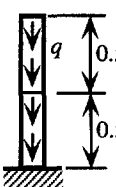
We point out that materials of the type considered in this paper are constructable. We offer only one simple example. Consider a closed pore foam; now pierce it throughout with parallel needles. The various physical parameters would be determined by the combination of pore volume fraction, pore geometry, concentration and diameter of punched holes, elastic properties of the skeleton, and viscosity and compressibility of the pore fluid. We also note that nature provides an example of such a material: the stems of herbaceous plants. Plant stems serve the dual function of providing structural strength and stiffness, and also contain the vascular tissue which conducts water from the root system to transpiring leaves. A crucial attribute to such plant elements is that their microstructure is designed to transport water axially. Thus one might model a living plant stem as a beam made up of a poroelastic material for which water movement in the axial direction is dominant when trying to understand the time dependent response of such elements to lateral (wind) loading.

#### REFERENCES

- Absousleiman, Y., Cheng, A. H.-D., Cui, L., Detournay, E. and Roegiers, J.-C. (1996) Mandel's Problem revisited. *Geotechnique* **46**, 187–195.
- Li, L. P., Cederbaum, G. and Schulgasser, K. (1996) Vibration of poroelastic beams with axial diffusion. *European Journal of Mechanics, A/Solids* **15**, 1077–1094.

Li, L. P., Cederbaum, G. and Schulgasser, K. (1997a) Theory of poroelastic plates with inplane diffusion. *International Journal of Solids and Structures* **34**, 4515–4530.  
 Li, L. P., Cederbaum, G. and Schulgasser, K. (1997b) A finite element model for poroelastic beams with axial diffusion, submitted.  
 Li, L. P., Schulgasser, K. and Cederbaum, G. (1995) Theory of poroelastic beams with axial diffusion. *Journal of the Mechanics and Physics of Solids* **43**, 202–204.  
 Mandel, J. (1953) Consolidation des sols (etude mathematique). *Geotechnique* **3**, 287–299.  
 Nowinski, J. L. and Davis, C. F. (1972) The flexure and torsion of bones viewed as anisotropic poroelastic bodies. *International Journal of Engineering Science* **10**, 1063–1079.  
 Terzaghi, K. (1943) *Theoretical Soil Mechanics*. New York, Wiley.  
 Zhang, D. and Cowin, S. C. (1994) Oscillatory bending of a poroelastic beam. *Journal of the Mechanics and Physics of Solids* **42**, 1575–1599.

APPENDIX: DETAILS OF LOADING CASES CONSIDERED

Figure	Loading	Remarks
2		$\lambda = \eta = 1$ $q = 1$
3		$\lambda = \eta = 1$ $q = 100$
4		$\lambda = \eta = 1$ $m = 1000$
5		$\lambda = 6, \eta = 1$ $q = 1$
6, 7		$\lambda = 6, \eta = 1$ $w = 1$
8		$\lambda = \eta = 1$ $q = -1$
9		$\eta = 1$ $q = -1$ $\lambda$ differs in two sections (see text)